



UWL REPOSITORY

repository.uwl.ac.uk

Classification of EEG signals for prediction of epileptic seizures

Aslam, Muhammad Haseeb, Usman, Syed Muhammad, Khalid, Shehzad, Anwar, Aamir, Alroobaea, Roobaea, Hussain, Saddam, Almotiri, Jasem, Ullah, Syed Sajid and Yasin, Amanullah (2022)

Classification of EEG signals for prediction of epileptic seizures. *Applied Sciences*, 12 (14). e7251.

<http://dx.doi.org/10.3390/app12147251>

This is the Published Version of the final output.

UWL repository link: <https://repository.uwl.ac.uk/id/eprint/9255/>

Alternative formats: If you require this document in an alternative format, please contact:

open.research@uwl.ac.uk

Copyright: Creative Commons: Attribution 4.0




Copyright and moral rights for the publications made accessible in the public portal are retained by the authors and/or other copyright owners and it is a condition of accessing publications that users recognise and abide by the legal requirements associated with these rights.

Take down policy: If you believe that this document breaches copyright, please contact us at

open.research@uwl.ac.uk providing details, and we will remove access to the work immediately and investigate your claim.

Article

Classification of EEG Signals for Prediction of Epileptic Seizures

Muhammad Haseeb Aslam ¹, Syed Muhammad Usman ², Shehzad Khalid ¹, Aamir Anwar ³ , Roobaea Alroobaea ⁴ , Saddam Hussain ^{5,*} , Jasem Almotiri ⁴, Syed Sajid Ullah ^{6,7,*} and Amanullah Yasin ²

- ¹ Department of Computer Engineering, Bahria University, Islamabad 44000, Pakistan; haseeb.aslam95.ha@gmail.com (M.H.A.); shehzad@bahria.edu.pk (S.K.)
 - ² Department of Creative Technologies, Faculty of Computing and Artificial Intelligence, Air University, Islamabad 44000, Pakistan; syed.usman@mail.au.edu.pk (S.M.U.); amanyasin@mail.au.edu.pk (A.Y.)
 - ³ School of Computing and Engineering, The University of West London, London W5 5RF, UK; 21452391@student.uwl.ac.uk
 - ⁴ Department of Computer Science, College of Computers and Information Technology, Taif University, P.O. Box 11099, Taif 21944, Saudi Arabia; r.robai@tu.edu.sa (R.A.); j.jasem@tu.edu.sa (J.A.)
 - ⁵ School of Digital Science, Universiti Brunei Darussalam, Jalan Tungku Link, Gadong, Seri Begawan BE1410, Brunei
 - ⁶ Department of Information and Communication Technology, University of Agder (UiA), N-4898 Grimstad, Norway
 - ⁷ Department of Electrical and Computer Engineering, Villanova University, Villanova, PA 19085, USA
- * Correspondence: saddamicup1993@gmail.com (S.H.); syed.s.ullah@uia.no (S.S.U.)

Abstract: Epilepsy is a common brain disorder that causes patients to face multiple seizures in a single day. Around 65 million people are affected by epilepsy worldwide. Patients with focal epilepsy can be treated with surgery, whereas generalized epileptic seizures can be managed with medications. It has been noted that in more than 30% of cases, these medications fail to control epileptic seizures, resulting in accidents and limiting the patient's life. Predicting epileptic seizures in such patients prior to the commencement of an oncoming seizure is critical so that the seizure can be treated with preventive medicines before it occurs. Electroencephalogram (EEG) signals of patients recorded to observe brain electrical activity during a seizure can be quite helpful in predicting seizures. Researchers have proposed methods that use machine and/or deep learning techniques to predict epileptic seizures using scalp EEG signals; however, prediction of seizures with increased accuracy is still a challenge. Therefore, we propose a three-step approach. It includes preprocessing of scalp EEG signals with PREP pipeline, which is a more sophisticated alternative to basic notch filtering. This method uses a regression-based technique to further enhance the SNR, with a combination of handcrafted, i.e., statistical features such as temporal mean, variance, and skewness, and automated features using CNN, followed by classification of interictal state and preictal state segments using LSTM to predict seizures. We train and validate our proposed technique on the CHB-MIT scalp EEG dataset and achieve accuracy of 94%, sensitivity of 93.8%, and 91.2% specificity. The proposed technique achieves better sensitivity and specificity than existing methods.

Keywords: epilepsy prediction; electroencephalogram; deep learning; preictal state; postictal state



Citation: Aslam, M.H.; Usman, S.M.; Khalid, S.; Anwar, A.; Alroobaea, R.; Hussain, S.; Almotiri, J.; Ullah, S.S.; Yasin, A. Classification of EEG Signals for Prediction of Epileptic Seizures. *Appl. Sci.* **2022**, *12*, 7251. <https://doi.org/10.3390/app12147251>

Academic Editor: Habib Hamam

Received: 4 June 2022

Accepted: 15 July 2022

Published: 19 July 2022

Publisher's Note: MDPI stays neutral with regard to jurisdictional claims in published maps and institutional affiliations.



Copyright: © 2022 by the authors. Licensee MDPI, Basel, Switzerland. This article is an open access article distributed under the terms and conditions of the Creative Commons Attribution (CC BY) license (<https://creativecommons.org/licenses/by/4.0/>).

1. Introduction

Patients experience seizures in epilepsy due to disruption in the functionality of neurons inside the brain. Around 65 million people worldwide are affected by epilepsy [1]. Conventional methods to treat epilepsy patients are through medication and surgery; however, successive seizures cannot be controlled using existing treatments in around 30% of patients [2]. Therefore, it is very important to predict subsequent seizures in time. Upcoming seizures, if detected early, can be stopped to avoid serious damage, which in some cases can be fatal. Mostly, such patients are monitored and examined using

electroencephalogram (EEG) recordings [3,4]. These recordings are then visually analyzed by doctors for a more comprehensive understanding of the patient's seizures. The procedure is subject to human error and is time consuming and highly subjective in nature. The need for an automatic seizure detection system arises, mainly aimed at accelerating the analysis process, making it accurate, and to assuage the workload of neurologists. EEG signals are recorded in two ways: one is scalp EEG, in which probes/electrodes are placed on the scalp of the subject, and the other is intracranial EEG, where EEG electrodes are fixed invasively on the tissues of the brain [5].

EEG signals of an epileptic patient can be broadly categorized into four states [6]: the preictal state [7] is the state a few minutes before the actual occurrence of the seizure; the ictal state [8] is the state when the seizure is actually occurring; the postictal state [9] is the state after the seizure has passed; and the interictal state is the state between two consecutive seizures, which can also be called the normal state. Figure 1 presents a multichannel plot of one hour of EEG signals. In seizure prediction, the preictal state is useful as it begins a few minutes prior to the seizure.

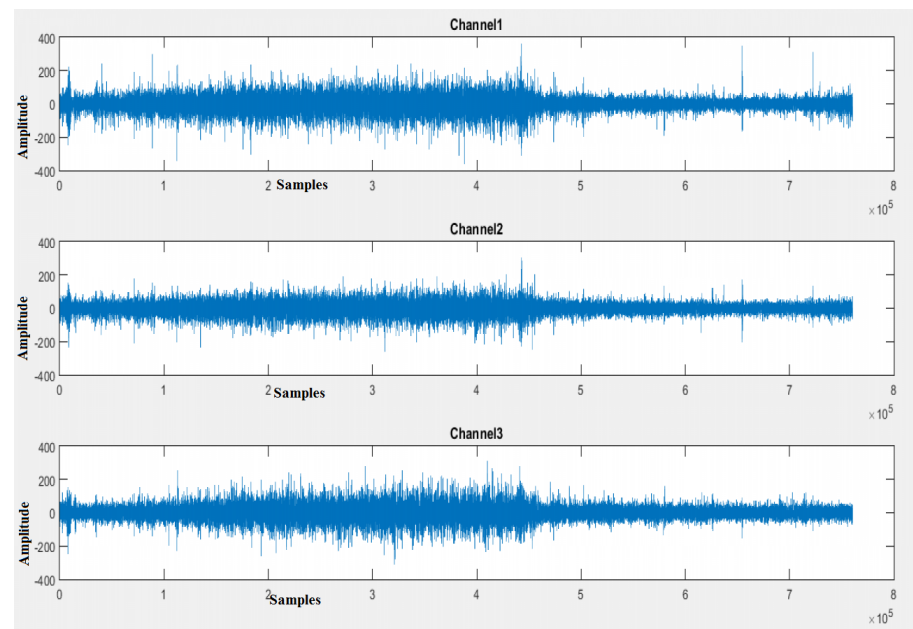


Figure 1. One hour recording of EEG signal of epileptic patient for three channels.

The preictal state is used for the detection and forecasting of seizures. It provides valuable information about the start of a seizure, as it begins a couple of minutes before the seizure actually occurs [6]. Predicting the ictal state by classifying the interictal and preictal state can help in averting seizures and the damage caused because of it by allowing timely administration of medicine. Figure 1 verifies the transformation in the electrical activity of the patient's brain between the preictal and the interictal states; in terms of both frequency and amplitude, there is an observable increase in the preictal state [10]. Prediction of epileptic seizures [11–35] includes preprocessing for noise reduction, feature set extraction, and categorization of interictal and preictal state segments. Inter-electrode interference, powerline noise, and noise owing to movement-related cortical potentials and ECG signals all cause noise in EEG signals during recording. Using machine learning and deep learning approaches, researchers have developed various ways for time/frequency domain extraction and automation. Automated features have been derived from many types of CNNs, whereas handcrafted features include time and frequency domain univariate and multivariate features. Machine learning classifiers such as SVM, decision tree, and MLP and deep learning-based classifiers such as CNN, RNN, and LSTM have been used to classify interictal and preictal state segments. Prediction accuracy remains a difficulty since it necessitates excellent preprocessing, features with large interclass variance, and improved

classification. We present a convolutional neural network and SVM-based technique for classification of EEG signals for epileptic seizure prediction in this research.

2. Related Work

Researchers [36–55] have proposed several techniques to predict seizures, including traditional machine learning approaches and deep learning techniques. EEG signals are generally susceptible to noise, especially scalp EEG, where electrodes that acquire the EEG signals are placed far from the source, i.e., on the scalp. Multiple types of noise affect the SNR of EEG signals, including powerline noise [56] between 50–60 Hz, baseline noise [57] that occurs because of the electrical interference of electrodes with each other, and artifacts that are generated because of human movements such as eye blink, pulse, etc. Researchers have proposed preprocessing techniques for increasing the signal-to-noise ratio (SNR) of electroencephalogram signals. The authors of [36,46,58] removed noise using bandpass filters. The authors of [38] transformed the time domain signals to frequency domain using fast Fourier transform (FFT). Researchers [39,59] have also used short time Fourier transform (STFT) to preprocess the EEG signals. STFT is very useful in preprocessing because of the non-stationary nature of EEG signals. The authors of [45] broke the signals down into multiple intrinsic mode functions (IMFs) on the basis of the frequency components using empirical mode decomposition (EMD) [60,61] as well as discrete wavelet transform (DWT) [62] for the purpose of preprocessing. In [41], the authors proposed DWT for preprocessing. Making a surrogate channel [63], using a common spatial pattern (CSP) [64], local mean decomposition (LMD) [60], or adaptive filtering [65] are some of the other ways of removing noise from EEGs.

Data after preprocessing is usually in large quantities and of a higher dimension. In this form, EEG signals are not suitable to be passed to classifier for classification. Therefore, a feature set is required, which is a subset of data that has lower dimensions and is not redundant. The process of converting data into a feature set is called feature extraction and extracts distinct features for classification. Both handcrafted and automated features have been extracted in existing methods. Handcrafted features of EEGs usually include univariate [66] and multivariate features [67]. Time domain features include Lyapunov exponent PCA [68], Hjorth parameters [69], approximate entropy [70], and statistical moments [71] and include the mean, also known as the average, variance, which is the deviation from the mean; skewness, which can be called distortion or asymmetry; kurtosis, which is the sharpness of the peak; and entropy, which is the measure of randomness in data [72]. Hjorth parameters are *complexity* and *mobility*. These parameters are helpful in the classification of EEG signals. Variance of the EEG signal through time is called Hjorth activity. The following equations give the mathematical representation of *activity*, *mobility*, and *complexity*, respectively.

$$Activity = var(y(t)) \quad (1)$$

$$Mobility(y(t)) = \sqrt{\frac{Activity(\frac{dy(t)}{dt})}{Activity(y(t))}} \quad (2)$$

$$Complexity(y(t)) = \frac{Mobility(\frac{dy(t)}{dt})}{Mobility(y(t))}. \quad (3)$$

Average frequency is given by *mobility*, whereas variation in frequency is given by *complexity*. Spectral features, which are frequency domain features, include spectral moments, spectral skewness, spectral centroid, variational coefficients, and power spectral density. Handcrafted features such as zero-crossings intervals [36], phase-locking values [45,46], bag of waves [37], and common spatial pattern filtering [44], have been extracted. Convolutional neural networks (CNNs) are used by [41,73] for feature extraction. A convolutional neural network extracts features in such a way that it keeps the class information; by doing this, features that have high inter-class variance are extracted. Ref. [74] used

Hilbert vibration decomposition for the extraction of amplitude modulation/frequency modulation subcomponents of signals of non-stationary nature.

Multiple traditional machine learning and a few cutting-edge deep learning methods have been employed for classification after extracting features. Machine learning classifiers include *k*-nearest neighbors (KNN) [69], naive Bayes [68], decision tree, and SVM. Deep learning-based classifiers include CNN, recurrent neural network (RNN), and long short-term memory (LSTM). Table 1 presents a comparison between these techniques along with their performance metrics results. Table 1 compares the existing state-of-the-art methods proposed in recent years. Preprocessing plays a vital role in achieving increased sensitivity when predicting an epileptic seizure. Moreover, extraction of multivariate features helps in getting better prediction results. Neural network-based classifiers and support vector machines seem to perform better than other classifiers. Average anticipation time and sensitivity are interrelated. If a prediction method has increased sensitivity, this leads to increased average anticipation time. However, wrong selection of a classification technique could lead to increased false positives and reduced sensitivity. Therefore, selection of the classifier can affect overall performance. In these studies, it is seen that damage due to epileptic seizures can be avoided by predicting the epileptic seizure through identifying the beginning of the preictal state. Effective preprocessing techniques are needed to remove that noise that was introduced in the acquisition of the EEG signal. Extracting and selecting features have also proven to be a major challenge.

Table 1. Preprocessing, feature extraction, and classifiers in existing methods.

Method	Preprocessing	Features	Classifier
[36]	Bandpass Filter	Zero Crossings	Variational GMM
[37]	-	Codebooks Construction, Bag of Waves Segmentation	ELM
[38]	Fast Fourier Transform	Spectral Features	Threshold for States
[39]	Short-Time Fourier Transform	Convolutional Neural Networks	Convolutional Neural Networks
[41]	Discrete Wavelet Transform	Convolutions Neural Network	Convolutional Neural Networks
[42]	Bandpass Filter	Lyapunov Exponent, Fourier Transform	Neural Networks
[43]	Derivatives and Statistical Moments	Derivative, Local Variance, Median Filtering	Thresholding
[44]	-	Statistical features using CSP	Linear Discriminant Analysis
[45]	Empirical Mode Decomposition	Phase Locking Value	Support Vector Machines
[46]	Standard Deviation/Bandpass Filter	Phase Locking Value	Thresholding
[74]	-	Hilbert Transform	Least Squares—Support Vector Machine

3. Overview of Proposed Method

We propose a patient-specific method for seizure prediction that predicts a seizure by detecting the start of preictal state. A flowchart for the proposed method is shown in Figure 2. The dataset used in this study is the widely used, publicly available CHB-MIT scalp EEG dataset [75]. It has recordings of 22 subjects with 23-channel signal recording and a sampling frequency of 256 Hz. PREP pipeline [76] is used to remove the powerline noise.

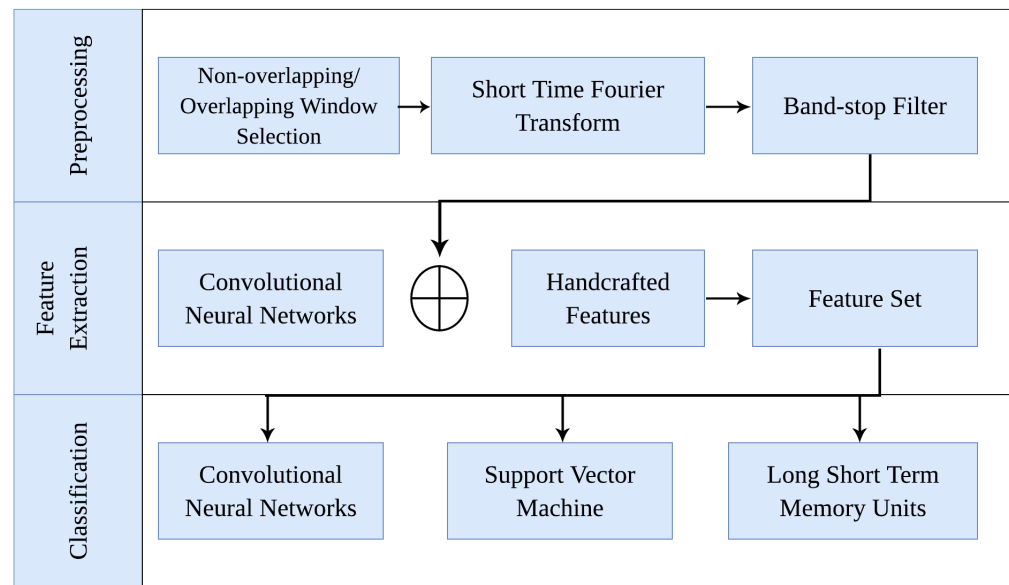


Figure 2. Flow diagram of the proposed epilepsy prediction system.

After noise is removed from the dataset, a sliding window of 30 s with 50% overlap is selected, and short time Fourier transform (STFT) is applied in order to further enhance the SNR and to convert from the time to frequency domain. The overlapping window is selected only in the preictal data. This is done to overcome the class imbalance between the interictal and preictal class. As stated earlier, the interictal state is the normal state of the brain, and the preictal state is recorded a few minutes before the occurrence of a seizure, so there is an inherent imbalance between the amount of data available for the two states. An overlapping window is used to perform oversampling of the preictal state. This is done across the board to all the channels and for each occurrence of preictal state. The interictal data is converted to frequency domain using a 30 s non-overlapping window. Figure 3 shows a visual representation of the overlapping and non-overlapping windows. Statistical moments have been extracted as handcrafted features, and CNN is applied for feature extraction. A custom, three-layer CNN is used that takes a $65 \times 117 \times 23$ matrix as the input size. Batch normalization is used to minimize internal covariate shift. Dense layers of the CNN architecture are removed. A feature vector containing both handcrafted and automated features has been created and given to the LSTM for classification.

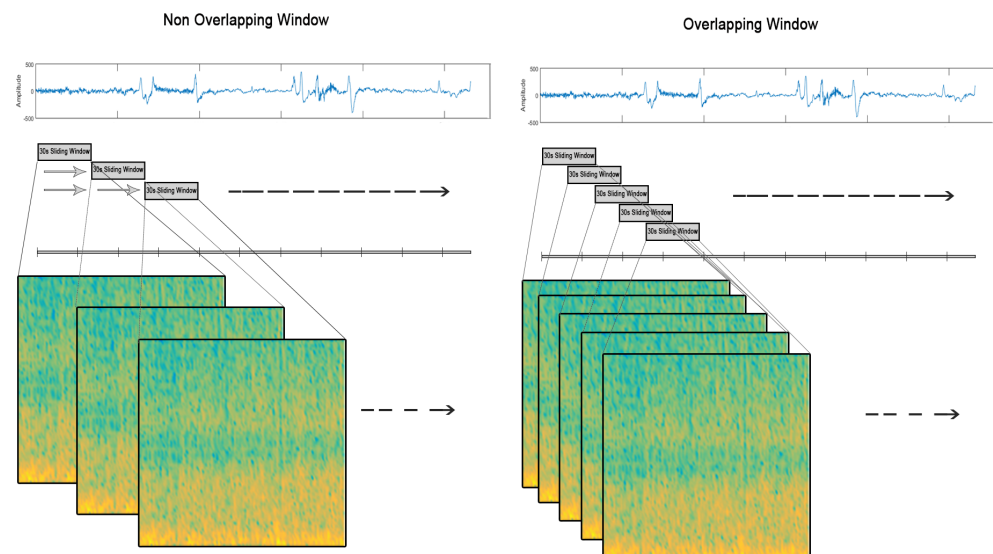


Figure 3. Non-overlapping/overlapping window selection.

4. Preprocessing

PREP pipeline can be summarized as: (1) Line-noise removal without restricting to a single filtering technique; (2) Robust referencing of the signal relative to an approximation of the “true” average reference; (3) Detection and interpolation of bad channels; and (4) Retention of sufficient data to allow users to use another method or to reverse interpolation of any channel. In theory, line noise is presumed to be at 60 Hz, but practically, the exact line frequency is unknown and variable. A regression model is applied across a range of frequencies centered on each potential line-noise frequency, and the line-noise frequency that maximizes the SNR is selected. This approach is advantageous over notch filtering because it only removes deterministic line components and preserves the spectral energy. Extensive testing proved that the line-noise removal algorithms did not yield good results if no high-pass filtering was done [76]. Thus, a high-pass filter at 1 Hz was applied before removing line-noise.

Short time Fourier transform (STFT) is used to transform EEG signals from the time to frequency domain. EEG signals are not stationary in nature, so STFT provides better results of preprocessing by capturing changes of short duration. In this study, we applied short term Fourier transform on a window of 30 for the data of the preictal state. The window used for preictal class was a 15 s overlap window, and a 30 s non-overlapping window was used for data of the interictal state to cater to the class imbalance problem. This conversion from time domain into frequency domain resulted in a spectrogram as shown in Figure 3. This spectrogram is given as input to the CNN to extract features.

5. Feature Extraction

Statistical moments have been extracted from all 23 channels as handcrafted features and include mean [77], standard deviation, and skewness [78], and are given by Equations (4)–(6), respectively.

$$\beta = \frac{1}{N} \sum_{i=1}^N (x_i - \mu)^3 \quad (4)$$

$$\sigma = \sqrt{\frac{1}{N} \sum_{i=1}^N (x_i - \mu)^2} \quad (5)$$

$$\mu = \frac{1}{N} \sum_{i=1}^N (x_i) \quad (6)$$

where x_i denotes the selected window of the EEG signal, and the total number of samples is given by N . After extraction of these handcrafted features, a custom CNN architecture was also used for feature extraction. CNNs are widely used for automated extraction of features and to classify time series and image data. Typical CNNs have multiple convolutional layers with different numbers of filters. Afterwards, the size of the layer is reduced by using a pooling layer that is then fed to fully connected layers used for classification. The last layer of such systems has neurons equal to the number of classes. Weight updating was as follows:

$$\Delta W_l(t+1) = -\frac{x\lambda}{r} W_l - \frac{x}{n} \left(\frac{\partial C}{\partial W_l} \right) + m \Delta W_l(t) \quad (7)$$

$$\Delta B_l(t+1) = -\frac{x}{n} \left(\frac{\partial C}{\partial B_l} \right) + m \Delta B_l(t). \quad (8)$$

Weight values are denoted by W , l represents the layer number, bias is denoted by B , and x and m are regularization parameters. After convolution, an activation function is used; some of the commonly used activation functions are rectified linear unit, sigmoid activation function, and the softmax activation function, and is computed using following equations.

$$y = \frac{1}{1 + e^{-x}} \quad (9)$$

$$\sigma(z) = \frac{e^z}{\sum_{i=1}^k e^{z_i}} \quad (10)$$

$$f(x) = \max(0, x). \quad (11)$$

A custom, three-layered CNN was proposed to extract machine-learned features. The first convolutional layer consists of 16 filters of 3×3 , the second layer has 32 filters of 3×3 , and the final convolutional layer is comprised of 64 filters of 3×3 . All these layers are followed by ReLU activation function and batch normalization. A flattened layer is then applied to get the machine-learned features to a size of 7192. Figure 4 presents the proposed architecture of the CNN, which consists of three layers of convolution, and the number of parameters to be trained in each layer is listed in Table 2.

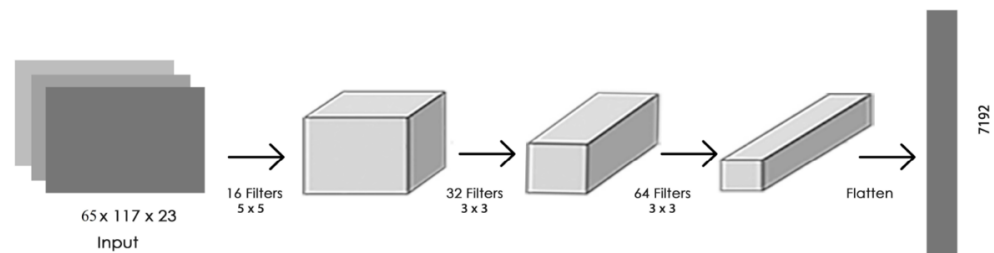


Figure 4. Proposed CNN.

Table 2. Model summary of convolutional neural network designed to extract features.

Layer Name	Output Shape	Parameters
conv2d (Conv2D)	(None, 65, 117, 16)	9216
maxpooling2d (MaxPooling2D)	(None, 32, 58, 16)	0
batch-normalization (BatchNo)	(None, 32, 58, 16)	64
conv2d1 (Conv2D)	(None, 32, 58, 32)	4640
maxpooling2d1 (MaxPooling2)	(None, 31, 57, 32)	0
batch-normalization1 (Batch No)	(None, 31, 57, 32)	128
conv2d2 (Conv2D)	(None, 31, 57, 64)	18,496
maxpooling2d2 (MaxPooling2)	(None, 30, 56, 64)	0
flatten (Flatten)	(None, 107,520)	0
dense (Dense)	(None, 256)	27,525,376
dense1 (Dense)	(None, 1)	257

6. Classification

For classification, we propose LSTM, a version of a recurrent neural network [79]. After concatenating statistics and CNN features, the combined feature set is transformed to a sequence length of 50 and fed into an LSTM for classification. The LSTM has many gates, including a forget gate and input gates, for storing and forgetting prior cell information. Forget ($f(t)$), input ($i(t)$), and previous LSTM layer (H_{t-1}) weights [80], plus cell states and new weights are computed as follows:

$$f(t) = \sigma(W_f \cdot [h_{t-1}, x_t] + b_f) \quad (12)$$

$$i(t) = \sigma(W_i \cdot [h_{t-1}, x_t] + b_i) \quad (13)$$

$$\hat{C}(t) = \tanh(W_C \cdot [h_{t-1}, x_t] + b_C) \quad (14)$$

$$C(t) = f_t * C_{t-1} + i_t * \hat{C}_t \quad (15)$$

$$o(t) = \sigma(W_o \cdot [h_{t-1}, x_t] + b_o) \quad (16)$$

$$h_t = o_t * \tanh(C_t) \quad (17)$$

The suggested method uses an LSTM with 256 neurons at the input and 02 neuron at the output to classify preictal state and interictal state EEG patterns. For classification using LSTM, the proposed approach includes 775,682 trainable parameters.

7. Results and Discussion

This study proposes a patient-specific seizure prediction system using data from 22 subjects, including 17 males and 5 females. Scalp EEG signals were used to classify between interictal, which is the normal EEG state, and preictal, which is the state a few minutes prior to the beginning of the seizure, states. Preictal class samples were labeled as the positive class, so it is imperative to achieve higher TPR and low false positives. Sensitivity and specificity have been used to validate the proposed method and are computed using the the following equations:

$$\text{Sensitivity} = \text{TP} / (\text{TP} + \text{FN}) \quad (18)$$

$$\text{Specificity} = \text{TN} / (\text{TN} + \text{FP}) \quad (19)$$

where TP stands for true positive, TN denotes true negative, FP is false positive, and FN represents false negative. The first experiment was devised to monitor the effects of different preprocessing techniques. Multiple experiments were performed to identify an optimal window size varying between 5 s to 120 s, and showed that a non-overlapping window of 30 s better characterizes the EEG signals. Therefore, a non-overlapping window (NOW) of 30 s was selected for both the interictal and preictal state segments. We then applied short time Fourier transform on the selected window, and no noise removal was done. Features were extracted using CNN, and the fully connected/dense layers at the end of the CNN were applied for classification. The results obtained in this setting are 64.5% sensitivity and 62.6% specificity.

In the second experimental setting, bandpass/bandstop filtering was applied to remove line noise in the preprocessing, while the rest of the settings were kept the same as in the previous experimental setup. We applied Butterworth bandstop filters from 47–53 Hz and 109–112 Hz to remove line noise. Butterworth bandstop filters give a maximally flat response. A high-pass filter was also applied at 1 Hz to remove the DC component. In this experiment, 72.4% sensitivity and 70.3% specificity were achieved. In the third experiment, the filter setting was kept the same, and the issue of class imbalance was targeted. There is a class imbalance issue in the dataset as the ratio of interictal and preictal class samples is 10:1. With the help of an overlapping window (OW) for preictal state segments with an overlap of 15 s, the ratio can be reduced to 5:1. This oversampling greatly improved the results. NOW for interictal and OW for preictal classes (15 s overlap), bandpass filtering, CNN for feature extraction, and ANN for classification yielded the best results, with 78.3% sensitivity and 76.1% specificity. These settings were kept constant in subsequent experiments. Table 3 shows the different experimental settings and the results achieved in each experiment.

Table 3. Results of various preprocessing techniques used in the proposed system.

Preprocessing	Feature Extraction	Classification	Sensitivity	Specificity
NOW interictal, preictal, STFT	CNN	ANN	64.5	62.6
NOW interictal–preictal, STFT, BPF/BSF	CNN	ANN	72.4	70.3
NOW interictal, OW preictal (15 s overlap), TFT, BPF/BSF	CNN	ANN	78.3	76.1

The second experiment was devised to select the best automated feature extraction model. In the first iteration, we kept the preprocessing settings the same as the first experiment and selected the state-of-the-art Resnet-50, a deep neural network with 50 layers, for feature extraction. Residual learning was also introduced using skip connections. After feature extraction, classification was done using fully-connected layers. The results

obtained using this approach were not comparable to the state-of-the-art. A sensitivity of 67.4% and a specificity of 54.3% was achieved. In the second iteration, a much smaller network, Visual Geometry Group-16 was used. In this iteration, the same settings were used as in the first iteration, with the only difference being the use of VGG-16 in place of Resnet. Similarly, ANN was used for classification. The results improved drastically with this change, and sensitivity of 87.3% and specificity of 83.2% were achieved. The results obtained using this setting were on par with the state-of-the-art systems, but to further enhance and analyze the effects of different feature extraction models, we designed a custom convolutional neural network with fewer layers. Similar architectures were also found in the literature after thorough study. The details of this network are explained in the Proposed Method section. The best results were achieved with this network, where a sensitivity of 89.3% and a specificity of 85.2% was achieved. This network was kept constant along with the preprocessing in the subsequent experiment. Table 4 shows the settings and the results achieved in each iteration in tabular form.

Table 4. Results of various feature extraction techniques used in the proposed system.

Preprocessing	Feature Extraction	Classification	Sensitivity	Specificity
NOW interictal OW preictal (15 s overlap) STFT BPF/BSF	Resnet-50	ANN	67.4	54.3
NOW interictal OW preictal (15 s overlap) STFT BPF/BSF	VGG-16	ANN	87.3	83.2
NOW interictal OW preictal (15 s overlap) STFT BPF/BSF	Custom-CNN	ANN	89.3	85.2

The third experiment was devised to analyze the efficiency of different classifiers. In this experiment, we fixed the two best settings from the previous experiments, i.e., non-overlapping window for the interictal class and overlapping window of 15 s for the preictal class, with STFT and bandpass/bandstop filtering and the custom CNN for feature extraction. In the first iteration, we used ANN, which is similar to the third iteration of Experiment 2. In the second iteration, we used decision tree and achieved sensitivity of 81.2% and specificity of 76.4%. In the third iteration, support vector machine was used after feature extraction. The results obtained by application of LSTM for classification were sensitivity of 92.8% and specificity of 90.7%. Table 5 shows the settings and the results achieved in each iteration in tabular form.

Different deep learning approaches were tried for automated feature extraction, including Resnet-101, Resnet-50, and VGG-16. Table 6 gives a comparison of these approaches with respect to sensitivity and specificity. Preprocessing was kept the same for all three experiment, with a non-overlapping window of 30 s for the interictal state and a 15 s overlapping window for the preictal state and PREP pipeline to remove the noise; k -fold cross-validation was applied for validation of results by keeping the value of $k = 10$. The proposed system achieved an average accuracy of 94%, 93.8% sensitivity, 91.2% specificity with standard deviation ranges between 1 to 1.5% for k folds in all performance measures. Table 7 shows the results of k -fold cross-validation achieved from the proposed method. An average prediction time of 19.5 min was achieved. Figure 5 and Table 8 compare the results of the proposed system with the current state-of-the-art systems. Singh et al. [52] achieved better results in terms of accuracy; however, they did not reported the average anticipation time, which is of prime importance in epilepsy prediction systems, as achieving greater accuracy with less time to control the seizure limits the usefulness of that method. Therefore, the proposed system performs better both in terms of specificity and sensitivity.

Table 5. Results of various classifiers used in the proposed system.

Preprocessing	Feature Extraction	Classification	Sensitivity	Specificity
NOW interictal OW preictal (15 s overlap) STFT BPF/BSF	Custom-CNN	ANN	89.34	85.4
NOW interictal OW preictal (15 s overlap) STFT BPF/BSF	Custom-CNN	DT	81.2	76.4
NOW interictal O.W preictal (15 s overlap) STFT BPF/BSF	Custom-CNN	LSTM	92.8	90.7

Table 6. Comparison of various deep learning models for feature extraction.

Feature Extraction	Sensitivity	Specificity
Resnet-101	68.4	59.6
Resnet 50	78.4	71.3
VGG-16	93.8	91.2

Table 7. The *k*-fold cross-validation results of the proposed method.

<i>k</i>	1	2	3	4	5	
Sensitivity (%)	93.3	93.7	94	93	94.2	
Specificity (%)	91	92	91	91.1	91.5	
<i>k</i>	6	7	8	9	10	Average
Sensitivity (%)	94.5	92.3	93.3	94.3	95.4	93.8
Specificity (%)	94.4	90	91	90	90	91.2

Table 8. Comparison of Sensitivity, Specificity and Average Anticipation time with recent techniques proposed by researchers.

Method	Sensitivity (%)	Specificity (%)	Average Prediction Time
[36]	83.8	83.5	19.8 min
[37]	70.5	75	1 min
[38]	86.7	86.67	45.3 min
[39]	81.2	84	5 min
[41]	87.8	85.8	-
[42]	89.5	89.75	-
[43]	90.3	85.2	22.63 min
[44]	81	61	38.35 min
[45]	80.54	80.50	-
[46]	76.8	90	-
[52]	98.51	97.78	-
[74]	89.0	80.2	-
Proposed Method	93.8	91.2	19.5 min

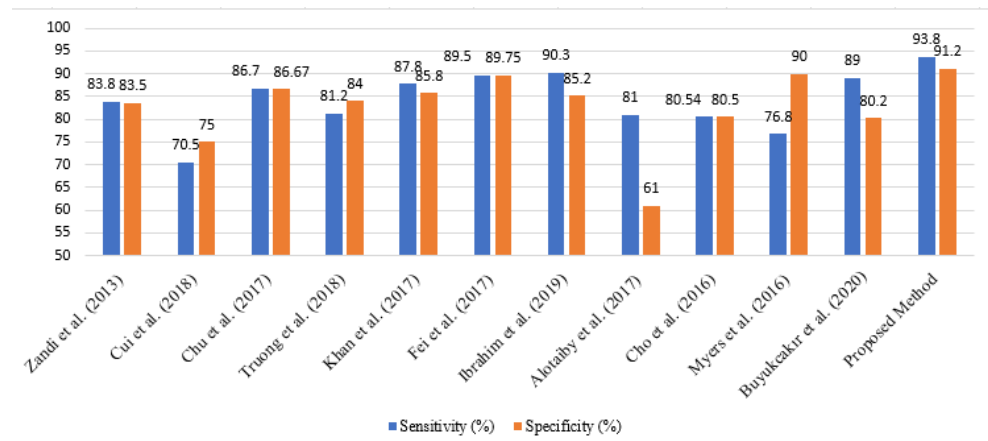


Figure 5. Comparison of results with recent techniques proposed by researchers [36–39,41–46,74].

The receiver operating characteristics curves of state-of-the-art systems and the proposed technique are shown in Figure 6. The sensitivity of the system is plotted against the FPR in these receiver operating characteristics curves to compare the overall performance of several state-of-the-art approaches. This allows us to determine whether or not the performance is satisfactory. If an increase in sensitivity does not result in an increase in false positive alarms, the system is said to be working well. The suggested system clearly beats the current state-of-the-art systems in terms of achieving high TPR with low FPR. It is concluded from the aforementioned evidence that the system proposed in this study is an effective seizure prediction method.

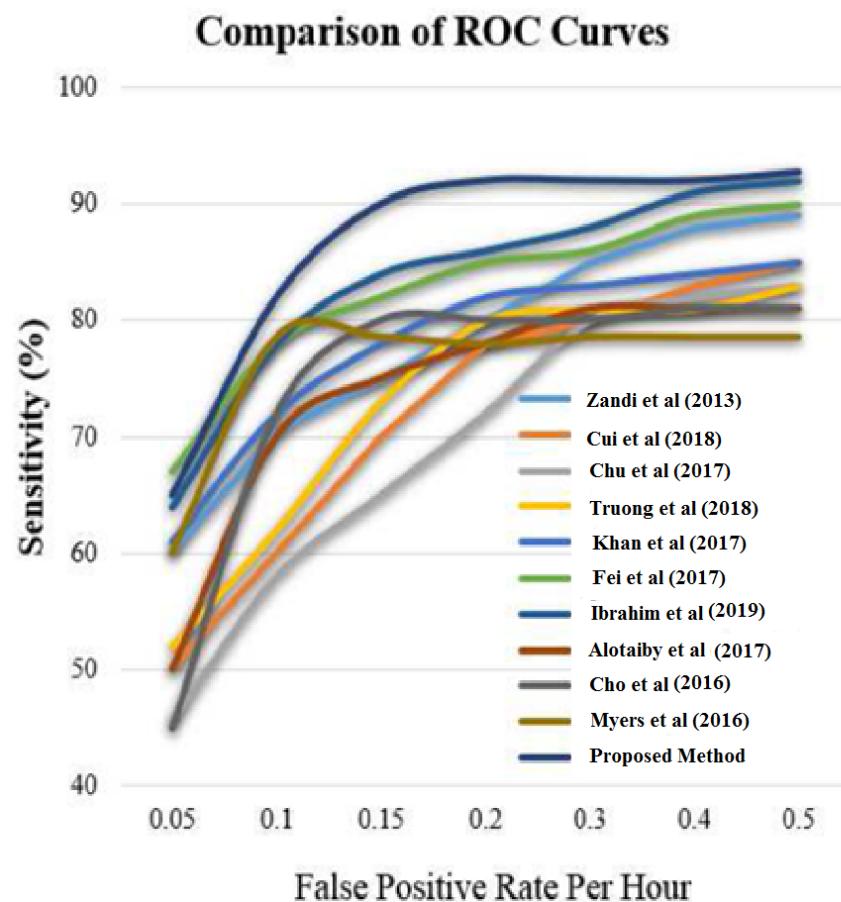


Figure 6. Analysis of ROC curves with existing methods [36–39,41–46,74].

8. Conclusions and Future Work

This research proposes a method for seizure prediction in epileptic patients using scalp EEG. Patients that have epilepsy can lead a risk-free life if timely and accurate seizure prediction is ensured. In comparison to existing methods, the proposed method uses a regression-based alternative to notch filtering to increase SNR, then combines automated feature extraction with CNN and handcrafted features and performs classification with an LSTM classifier to achieve better sensitivity and specificity. The model was trained and validated on the CHB-MIT scalp EEG dataset, and it achieved 94% accuracy, 93.8% sensitivity, and 91.2% specificity. In the future, intelligent algorithms such as CNN and GAN-based denoising methods [49] can be used to preprocess the data to further increase the SNR. From the deep learning aspect, large numbers of parameters need to be learned; research can be done to make the algorithms more efficient by reducing the number of operations and learnable parameters, which will lead to less-computationally intense models. This study proposes patient-specific seizure prediction; a lot of research can be done to develop a patient nonspecific seizure prediction method.

Author Contributions: Conceptualization, M.H.A., S.M.U., S.K., J.A. and R.A.; methodology, M.H.A., S.M.U., S.K., A.A. and J.A.; software, M.H.A., A.A. and A.Y.; validation, M.H.A. and A.Y.; formal analysis, S.M.U., S.K., A.A. and A.Y.; investigation, S.M.U., S.K., S.H., S.S.U., A.Y.; resources, R.A., S.H., J.A., S.S.U. and A.Y.; data curation, S.M.U.; writing—original draft preparation, M.H.A.; writing—review and editing, S.M.U., S.K., A.Y.; visualization, A.A., R.A., S.H. and S.S.U.; supervision, S.M.U. and S.K.; project administration, S.K., J.A. and R.A.; funding acquisition, R.A. and J.A. All authors have read and agreed to the published version of the manuscript.

Funding: The authors are grateful to the Taif University Researchers Supporting Project number (TURSP-2020/36), Taif University, Taif, Saudi Arabia.

Institutional Review Board Statement: Not Applicable.

Informed Consent Statement: Not Applicable.

Conflicts of Interest: The authors declare no conflict of interest.

References

1. Cook, M.J.; O'Brien, T.J.; Berkovic, S.F.; Murphy, M.; Morokoff, A.; Fabinyi, G.; D'Souza, W.; Yerra, R.; Archer, J.; Litewka, L.; et al. Prediction of seizure likelihood with a long-term, implanted seizure advisory system in patients with drug-resistant epilepsy: A first-in-man study. *Lancet Neurol.* **2013**, *12*, 563–571. [\[CrossRef\]](#)
2. Devarajan, K.; Jyostna, E.; Jayasri, K.; Balasampath, V. EEG-based epilepsy detection and prediction. *Int. J. Eng. Technol.* **2014**, *6*, 212–216. [\[CrossRef\]](#)
3. Abdulghani, A.M.; Casson, A.J.; Rodriguez-Villegas, E. Compressive sensing scalp EEG signals: Implementations and practical performance. *Med. Biol. Eng. Comput.* **2012**, *50*, 1137–1145. [\[CrossRef\]](#) [\[PubMed\]](#)
4. Chávez, M.; Martinerie, J.; Le Van Quyen, M. Statistical assessment of nonlinear causality: Application to epileptic EEG signals. *J. Neurosci. Methods* **2003**, *124*, 113–128. [\[CrossRef\]](#)
5. Le Van Quyen, M.; Martinerie, J.; Navarro, V.; Boon, P.; D'Havé, M.; Adam, C.; Renault, B.; Varela, F.; Baulac, M. Anticipation of epileptic seizures from standard EEG recordings. *Lancet* **2001**, *357*, 183–188. [\[CrossRef\]](#)
6. Robinson, P.; Rennie, C.; Rowe, D. Dynamics of large-scale brain activity in normal arousal states and epileptic seizures. *Phys. Rev. E* **2002**, *65*, 041924. [\[CrossRef\]](#)
7. Ghosh-Dastidar, S.; Adeli, H.; Dadmehr, N. Mixed-band wavelet-chaos-neural network methodology for epilepsy and epileptic seizure detection. *IEEE Trans. Biomed. Eng.* **2007**, *54*, 1545–1551. [\[CrossRef\]](#)
8. Schuyler, R.; White, A.; Staley, K.; Cios, K.J. Epileptic seizure detection. *IEEE Eng. Med. Biol. Mag.* **2007**, *26*, 74. [\[CrossRef\]](#)
9. Fisher, R.S.; Engel, J.J., Jr. Definition of the postictal state: When does it start and end? *Epilepsy Behav.* **2010**, *19*, 100–104. [\[CrossRef\]](#)
10. Hazarika, N.; Chen, J.Z.; Tsoi, A.C.; Sergejew, A. Classification of EEG signals using the wavelet transform. *Signal Process.* **1997**, *59*, 61–72. [\[CrossRef\]](#)
11. Iasemidis, L.D. Epileptic seizure prediction and control. *IEEE Trans. Biomed. Eng.* **2003**, *50*, 549–558. [\[CrossRef\]](#)
12. Yu, H.; Fan, C.; Zhang, Y. Epilepsy Detection in EEG Using Grassmann Discriminant Analysis Method. *Comput. Math. Methods Med.* **2020**, *2020*, 2598140. [\[CrossRef\]](#)
13. Nasser, M.; Kremen, V.; Nejedly, P.; Kim, I.; Chang, S.Y.; Jo, H.J.; Guragain, H.; Nelson, N.; Patterson, E.; Sturges, B.K.; et al. Semi-supervised training data selection improves seizure forecasting in canines with epilepsy. *Biomed. Signal Process. Control* **2020**, *57*, 101743. [\[CrossRef\]](#)

14. Das, K.; Daschakladar, D.; Roy, P.P.; Chatterjee, A.; Saha, S.P. Epileptic seizure prediction by the detection of seizure waveform from the pre-ictal phase of EEG signal. *Biomed. Signal Process. Control* **2020**, *57*, 101720. [\[CrossRef\]](#)
15. Ozcan, A.R.; Erturk, S. Seizure Prediction in Scalp EEG Using 3D Convolutional Neural Networks With an Image-Based Approach. *IEEE Trans. Neural Syst. Rehabil. Eng.* **2019**, *27*, 2284–2293. [\[CrossRef\]](#)
16. Tsipouras, M.G. Spectral information of EEG signals with respect to epilepsy classification. *EURASIP J. Adv. Signal Process.* **2019**, *2019*, 10. [\[CrossRef\]](#)
17. Usman, S.M.; Hassan, A. Efficient Prediction and Classification of Epileptic Seizures Using EEG Data Based on Univariate Linear Features. *JCP* **2018**, *13*, 616–621. [\[CrossRef\]](#)
18. Sudalaimani, C.; Sivakumaran, N.; Elizabeth, T.T.; Rominus, V.S. Automated detection of the pre-seizure state in EEG signal using neural networks. *Biocybern. Biomed. Eng.* **2019**, *39*, 160–175. [\[CrossRef\]](#)
19. Quintero-Rincón, A.; Pereyra, M.; d’Giano, C.; Risk, M.; Batatia, H. Fast statistical model-based classification of epileptic EEG signals. *Biocybern. Biomed. Eng.* **2018**, *38*, 877–889. [\[CrossRef\]](#)
20. Zhou, M.; Tian, C.; Cao, R.; Wang, B.; Niu, Y.; Hu, T.; Guo, H.; Xiang, J. Epileptic seizure detection based on EEG signals and CNN. *Front. Neuroinformatics* **2018**, *12*, 95. [\[CrossRef\]](#)
21. Usman, S.M.; Khalid, S.; Aslam, M.H. Epileptic Seizures Prediction Using Deep Learning Techniques. *IEEE Access* **2020**, *8*, 39998–40007. [\[CrossRef\]](#)
22. Ibrahim, S.; Djemal, R.; Alsulwaleem, A. Electroencephalography (EEG) signal processing for epilepsy and autism spectrum disorder diagnosis. *Biocybern. Biomed. Eng.* **2018**, *38*, 16–26. [\[CrossRef\]](#)
23. Zhang, T.; Chen, W.; Li, M. Generalized Stockwell transform and SVD-based epileptic seizure detection in EEG using random forest. *Biocybern. Biomed. Eng.* **2018**, *38*, 519–534. [\[CrossRef\]](#)
24. Yavuz, E.; Kasapbaşı, M.C.; Eyüpoğlu, C.; Yazıcı, R. An epileptic seizure detection system based on cepstral analysis and generalized regression neural network. *Biocybern. Biomed. Eng.* **2018**, *38*, 201–216. [\[CrossRef\]](#)
25. Li, M.; Chen, W.; Zhang, T. Application of MODWT and log-normal distribution model for automatic epilepsy identification. *Biocybern. Biomed. Eng.* **2017**, *37*, 679–689. [\[CrossRef\]](#)
26. Swami, P.; Gandhi, T.K.; Panigrahi, B.K.; Tripathi, M.; Anand, S. A novel robust diagnostic model to detect seizures in electroencephalography. *Expert Syst. Appl.* **2016**, *56*, 116–130. [\[CrossRef\]](#)
27. Usman, S.M.; Khalid, S.; Akhtar, R.; Bortolotto, Z.; Bashir, Z.; Qiu, H. Using scalp EEG and intracranial EEG signals for predicting epileptic seizures: Review of available methodologies. *Seizure* **2019**, *71*, 258–269. [\[CrossRef\]](#)
28. Winterhalder, M.; Maiwald, T.; Voss, H.; Aschenbrenner-Scheibe, R.; Timmer, J.; Schulze-Bonhage, A. The seizure prediction characteristic: A general framework to assess and compare seizure prediction methods. *Epilepsy Behav.* **2003**, *4*, 318–325. [\[CrossRef\]](#)
29. Usman, S.M.; Khalid, S.; Bashir, Z. Epileptic seizure prediction using scalp electroencephalogram signals. *Biocybern. Biomed. Eng.* **2021**, *41*, 211–220. [\[CrossRef\]](#)
30. Carney, P.R.; Myers, S.; Geyer, J.D. Seizure prediction: Methods. *Epilepsy Behav.* **2011**, *22*, S94–S101. [\[CrossRef\]](#)
31. Acharya, U.R.; Oh, S.L.; Hagiwara, Y.; Tan, J.H.; Adeli, H.; Subha, D.P. Automated EEG-based screening of depression using deep convolutional neural network. *Comput. Methods Programs Biomed.* **2018**, *161*, 103–113. [\[CrossRef\]](#) [\[PubMed\]](#)
32. Ramgopal, S.; Thome-Souza, S.; Jackson, M.; Kadish, N.E.; Fernández, I.S.; Klehm, J.; Bosl, W.; Reinsberger, C.; Schachter, S.; Loddenkemper, T. Seizure detection, seizure prediction, and closed-loop warning systems in epilepsy. *Epilepsy Behav.* **2014**, *37*, 291–307. [\[CrossRef\]](#) [\[PubMed\]](#)
33. DuBois, J.; Boylan, L.; Shiyko, M.; Barr, W.; Devinsky, O. Seizure prediction and recall. *Epilepsy Behav.* **2010**, *18*, 106–109. [\[CrossRef\]](#) [\[PubMed\]](#)
34. Bandarabadi, M.; Rasekhi, J.; Teixeira, C.A.; Karami, M.R.; Dourado, A. On the proper selection of preictal period for seizure prediction. *Epilepsy Behav.* **2015**, *46*, 158–166. [\[CrossRef\]](#)
35. Usman, S.M.; Usman, M.; Fong, S. Epileptic Seizures Prediction Using Machine Learning Methods. *Comput. Math. Methods Med.* **2017**, *2017*, 9074759. [\[CrossRef\]](#)
36. Zandi, A.S.; Tafreshi, R.; Javidan, M.; Dumont, G.A. Predicting epileptic seizures in scalp EEG based on a variational Bayesian Gaussian mixture model of zero-crossing intervals. *IEEE Trans. Biomed. Eng.* **2013**, *60*, 1401–1413. [\[CrossRef\]](#)
37. Cui, S.; Duan, L.; Qiao, Y.; Xiao, Y. Learning EEG synchronization patterns for epileptic seizure prediction using bag-of-wave features. *J. Ambient. Intell. Humaniz. Comput.* **2018**, 1–16. [\[CrossRef\]](#)
38. Chu, H.; Chung, C.K.; Jeong, W.; Cho, K.H. Predicting epileptic seizures from scalp EEG based on attractor state analysis. *Comput. Methods Programs Biomed.* **2017**, *143*, 75–87. [\[CrossRef\]](#)
39. Truong, N.D.; Nguyen, A.D.; Kuhlmann, L.; Bonyadi, M.R.; Yang, J.; Ippolito, S.; Kavehei, O. Convolutional neural networks for seizure prediction using intracranial and scalp electroencephalogram. *Neural Netw.* **2018**, *105*, 104–111. [\[CrossRef\]](#)
40. Usman, S.M.; Khalid, S.; Bashir, S. A deep learning based ensemble learning method for epileptic seizure prediction. *Comput. Biol. Med.* **2021**, *136*, 104710. [\[CrossRef\]](#)
41. Khan, H.; Marcuse, L.; Fields, M.; Swann, K.; Yener, B. Focal onset seizure prediction using convolutional networks. *IEEE Trans. Biomed. Eng.* **2017**, *65*, 2109–2118. [\[CrossRef\]](#)
42. Fei, K.; Wang, W.; Yang, Q.; Tang, S. Chaos feature study in fractional Fourier domain for preictal prediction of epileptic seizure. *Neurocomputing* **2017**, *249*, 290–298. [\[CrossRef\]](#)

43. Ibrahim, F.; El-Gindy, S.A.E.; El-Dolil, S.M.; El-Fishawy, A.S.; El-Rabaie, E.S.M.; Dessouky, M.I.; Eldokany, I.M.; Alotaiby, T.N.; Alshebeili, S.A.; El-Samie, F.E.A. A statistical framework for EEG channel selection and seizure prediction on mobile. *Int. J. Speech Technol.* **2019**, *22*, 191–203. [\[CrossRef\]](#)
44. Alotaiby, T.N.; Alshebeili, S.A.; Alotaibi, F.M.; Alrshoud, S.R. Epileptic seizure prediction using CSP and LDA for scalp EEG signals. *Comput. Intell. Neurosci.* **2017**, *2017*, 1240323. [\[CrossRef\]](#)
45. Cho, D.; Min, B.; Kim, J.; Lee, B. EEG-based prediction of epileptic seizures using phase synchronization elicited from noise-assisted multivariate empirical mode decomposition. *IEEE Trans. Neural Syst. Rehabil. Eng.* **2016**, *25*, 1309–1318. [\[CrossRef\]](#)
46. Myers, M.H.; Padmanabha, A.; Hossain, G.; de Jongh Curry, A.L.; Blaha, C.D. Seizure prediction and detection via phase and amplitude lock values. *Front. Hum. Neurosci.* **2016**, *10*, 80. [\[CrossRef\]](#)
47. Mutlu, A.Y. Detection of epileptic dysfunctions in EEG signals using Hilbert vibration decomposition. *Biomed. Signal Process. Control* **2018**, *40*, 33–40. [\[CrossRef\]](#)
48. Slimen, I.B.; Boubchir, L.; Mbarki, Z.; Seddik, H. EEG epileptic seizure detection and classification based on dual-tree complex wavelet transform and machine learning algorithms. *J. Biomed. Res.* **2020**, *34*, 151. [\[CrossRef\]](#)
49. Mukherjee, S.; Kottayil, N.K.; Sun, X.; Cheng, I. CNN-Based Real-Time Parameter Tuning for Optimizing Denoising Filter Performance. In Proceedings of the International Conference on Image Analysis and Recognition, Waterloo, ON, Canada, 27–29 August 2019; Springer: Berlin/Heidelberg, Germany, 2019; pp. 112–125.
50. Malekzadeh, A.; Zare, A.; Yaghoobi, M.; Kobravi, H.R.; Alizadehsani, R. Epileptic Seizures Detection in EEG Signals Using Fusion Handcrafted and Deep Learning Features. *Sensors* **2021**, *21*, 7710. [\[CrossRef\]](#)
51. Shoeibi, A.; Ghassemi, N.; Khodatars, M.; Moridian, P.; Alizadehsani, R.; Zare, A.; Khosravi, A.; Subasi, A.; Acharya, U.R.; Gorriz, J.M. Detection of epileptic seizures on EEG signals using ANFIS classifier, autoencoders and fuzzy entropies. *Biomed. Signal Process. Control* **2022**, *73*, 103417. [\[CrossRef\]](#)
52. Singh, K.; Malhotra, J. Two-layer LSTM network-based prediction of epileptic seizures using EEG spectral features. *Complex Intell. Syst.* **2022**, *8*, 2405–2418. [\[CrossRef\]](#)
53. Tuncer, E.; Bolat, E.D. Classification of epileptic seizures from electroencephalogram (EEG) data using bidirectional short-term memory (Bi-LSTM) network architecture. *Biomed. Signal Process. Control* **2022**, *73*, 103462. [\[CrossRef\]](#)
54. Malekzadeh, A.; Zare, A.; Yaghoobi, M.; Alizadehsani, R. Automatic Diagnosis of Epileptic Seizures in EEG Signals Using Fractal Dimension Features and Convolutional Autoencoder Method. *Big Data Cogn. Comput.* **2021**, *5*, 78. [\[CrossRef\]](#)
55. Guo, Y.; Jiang, X.; Tao, L.; Meng, L.; Dai, C.; Long, X.; Wan, F.; Zhang, Y.; Van Dijk, J.; Aarts, R.M.; et al. Epileptic Seizure Detection by Cascading Isolation Forest-Based Anomaly Screening and EasyEnsemble. *IEEE Trans. Neural Syst. Rehabil. Eng.* **2022**, *30*, 915–924. [\[CrossRef\]](#)
56. Reddy, A.G.; Narava, S. Artifact removal from EEG signals. *Int. J. Comput. Appl.* **2013**, *77*, 17–19.
57. Traub, R.D.; Jefferys, J.G. Are there unifying principles underlying the generation of epileptic afterdischarges in vitro? *Prog. Brain Res.* **1994**, *102*, 383–394.
58. Delorme, A.; Sejnowski, T.; Makeig, S. Enhanced detection of artifacts in EEG data using higher-order statistics and independent component analysis. *Neuroimage* **2007**, *34*, 1443–1449. [\[CrossRef\]](#)
59. Meenakshi, D.; Singh, A.; Singh, A. Frequency analysis of healthy & epileptic seizure in EEG using fast Fourier transform. *Int. J. Eng. Res. Gen. Sci.* **2014**, *2*, 683–691.
60. Pachori, R.B.; Bajaj, V. Analysis of normal and epileptic seizure EEG signals using empirical mode decomposition. *Comput. Methods Programs Biomed.* **2011**, *104*, 373–381. [\[CrossRef\]](#)
61. Usman, S.M.; Khalid, S.; Jabbar, S.; Bashir, S. Detection of preictal state in epileptic seizures using ensemble classifier. *Epilepsy Res.* **2021**, *178*, 106818. [\[CrossRef\]](#)
62. Panda, R.; Khobragade, P.; Jambhule, P.; Jengthe, S.; Pal, P.; Gandhi, T. Classification of EEG signal using wavelet transform and support vector machine for epileptic seizure diction. In Proceedings of the 2010 International Conference on Systems in Medicine and Biology (ICSMB), Kharagpur, India, 16–18 December 2010; IEEE: Piscataway, NJ, USA, 2010; pp. 405–408.
63. Korff, C.M.; Brunklaus, A.; Zuberi, S.M. Epileptic activity is a surrogate for an underlying etiology and stopping the activity has a limited impact on developmental outcome. *Epilepsia* **2015**, *56*, 1477–1481. [\[CrossRef\]](#) [\[PubMed\]](#)
64. Zheng, G.; Yu, L.; Feng, Y.; Han, Z.; Chen, L.; Zhang, S.; Wang, D.; Han, Z. Seizure prediction model based on method of common spatial patterns and support vector machine. In Proceedings of the 2012 International Conference on the Information Science and Technology (ICIST), Wuhan, China, 23–25 March 2012; IEEE: Piscataway, NJ, USA, 2012; pp. 29–34.
65. Padmasai, Y.; SubbaRao, K.; Malini, V.; Rao, C.R. Linear prediction modelling for the analysis of the epileptic EEG. In Proceedings of the 2010 International Conference on Advances in Computer Engineering, Bangalore, India, 20–21 June 2010; IEEE: Piscataway, NJ, USA, 2010; pp. 6–9.
66. Otoum, S.; Kantarci, B.; Mouftah, H.T. On the feasibility of deep learning in sensor network intrusion detection. *IEEE Netw. Lett.* **2019**, *1*, 68–71. [\[CrossRef\]](#)
67. Faust, O.; Hagiwara, Y.; Hong, T.J.; Lih, O.S.; Acharya, U.R. Deep learning for healthcare applications based on physiological signals: A review. *Comput. Methods Programs Biomed.* **2018**, *161*, 1–13. [\[CrossRef\]](#) [\[PubMed\]](#)
68. Sharmila, A.; Geethanjali, P. DWT based detection of epileptic seizure from EEG signals using naive Bayes and k-NN classifiers. *IEEE Access* **2016**, *4*, 7716–7727. [\[CrossRef\]](#)

69. Chaovalitwongse, W.A.; Fan, Y.J.; Sachdeo, R.C. On the time series k -nearest neighbor classification of abnormal brain activity. *IEEE Trans. Syst. Man Cybern. Part A Syst. Hum.* **2007**, *37*, 1005–1016. [\[CrossRef\]](#)
70. Bajaj, V.; Pachori, R.B. Classification of seizure and nonseizure EEG signals using empirical mode decomposition. *IEEE Trans. Inf. Technol. Biomed.* **2011**, *16*, 1135–1142. [\[CrossRef\]](#)
71. Korshunova, I.; Kindermans, P.J.; Degrave, J.; Verhoeven, T.; Brinkmann, B.H.; Dambre, J. Towards improved design and evaluation of epileptic seizure predictors. *IEEE Trans. Biomed. Eng.* **2017**, *65*, 502–510. [\[CrossRef\]](#)
72. Khan, M.Z.; Naseem, R.; Anwar, A.; Haq, I.U.; Alturki, A.; Ullah, S.S.; Al-Hadhrani, S.A. A novel approach to automate complex software modularization using a fact extraction system. *J. Math.* **2022**, *2022*, 8640596. [\[CrossRef\]](#)
73. Haq, I.U.; Anwar, A.; Basharat, I.; Sultan, K. Intelligent Tutoring Supported Collaborative Learning (ITSCL): A Hybrid Framework. *Int. J. Adv. Comput. Sci. Appl.* **2020**, *11*, 523–535. [\[CrossRef\]](#)
74. Büyükçakır, B.; Elmaz, F.; Mutlu, A.Y. Hilbert vibration decomposition-based epileptic seizure prediction with neural network. *Comput. Biol. Med.* **2020**, *119*, 103665. [\[CrossRef\]](#)
75. Goldberger, A.L.; Amaral, L.A.; Glass, L.; Hausdorff, J.M.; Ivanov, P.C.; Mark, R.G.; Mietus, J.E.; Moody, G.B.; Peng, C.K.; Stanley, H.E. PhysioBank, PhysioToolkit, and PhysioNet: Components of a new research resource for complex physiologic signals. *Circulation* **2000**, *101*, e215–e220. [\[CrossRef\]](#)
76. Bigdely-Shamlo, N.; Mullen, T.; Kothe, C.; Su, K.M.; Robbins, K.A. The PREP pipeline: Standardized preprocessing for large-scale EEG analysis. *Front. Neuroinformatics* **2015**, *9*, 16. [\[CrossRef\]](#)
77. Sun, M.; Wang, F.; Min, T.; Zang, T.; Wang, Y. Prediction for high risk clinical symptoms of epilepsy based on deep learning algorithm. *IEEE Access* **2018**, *6*, 77596–77605. [\[CrossRef\]](#)
78. Nejedly, P.; Kremen, V.; Sladky, V.; Nasser, M.; Guragain, H.; Klimes, P.; Cimbalnik, J.; Varatharajah, Y.; Brinkmann, B.H.; Worrell, G.A. Deep-learning for seizure forecasting in canines with epilepsy. *J. Neural Eng.* **2019**, *16*, 036031. [\[CrossRef\]](#)
79. Yildirim, O.; Baloglu, U.B.; Tan, R.S.; Ciaccio, E.J.; Acharya, U.R. A new approach for arrhythmia classification using deep coded features and LSTM networks. *Comput. Methods Programs Biomed.* **2019**, *176*, 121–133. [\[CrossRef\]](#)
80. Stollenga, M.F.; Byeon, W.; Liwicki, M.; Schmidhuber, J. Parallel multi-dimensional lstm, with application to fast biomedical volumetric image segmentation. *Adv. Neural Inf. Process. Syst.* **2015**, *28*, 2998–3006.